Available online at www.sciencedirect.com

ScienceDirect

Procedia Structural Integrity 14 (2019) 34–43

Structural Integrity Procedia

www.elsevier.com/locate/procedia

2nd International Conference on Structural Integrity and Exhibition 2018

Characteristics of strain-induced martensitic transformation in welded joints with the structure of metastable austenite

Korobov Iu., Pimenova O., Filippov M., Khadyev M., Ozerets N., Mikhailov S., Morozov S., Davydov Iu., Razikov N.*

Ural Federal University, 19 Mira str., Ekaterinburg, 620002, Russia

Abstract

Welded joints of medium-carbon steel were performed by arc welding in shielding gases using cored wire of 50Cr18 type. Phase transitions in the process of crystallization and subsequent thermal and deformation effects under loading were studied. For this purpose, the weldability, wear resistant tests and structure study results were analyzed. It was found that the structure contains an increased amount of metastable austenite, δ-ferrite and high-strength carbonaceous-chromic martensite. Welded joints have a high capacity for intensive hardening during local deformation due to the TRIP effect. At the same time, they are highly resistant against the formation of cold cracks, which is the main defect in the welds of medium-carbon steels. It was shown that these features are reasoned from the heterophase dissipative structure of the weld metal formed under the conditions of a typical thermal-deformation cycle of the welded joint.

Keywords: Type your keywords here, separated by semicolons ;

* Corresponding author. Tel.: +7-919-379-2016; fax: +7-343-375-9569.
E-mail address: yukorobov@gmail.com

10.1016/j.prostr.2019.05.006

1. Introduction

High tensile strength, 1500-2200 MPa, and hardness, 477-534 HB, characterize medium-alloyed high-strength steels after heat treatment. This allows them to cover restriction on the mass of structures and requirements for wear resistance and other mechanical effects. They are used in automobile industry, shipbuilding, aviation, etc. The main method of connecting individual elements to these structures is welding. However, there is no an integrated solution for the following problems:

1) Weldability of high-strength steels of this class is limited mainly due to the propensity to cold cracking. The reason is the insufficient deformation ability of the metal at a sharp change of the strains during phase and structural transformations. To date, a set of material, structural and technological solutions has been developed to increase the resistance of high-strength steels against the cold cracking during welding.

2) The welds are exposed to wear and various external actions. However, ferrite-pearlitic and austenitic welding wires adopted in the normative documents do not provide the required resistance against these loads.

To solve these problems jointly, it is promising to have a structure of metastable austenite (MSA) in the weld. The popularity for applications of MSA containing steels as smart materials is related to its self-accommodation. Microtrip effect is realized in MSA steels due to controlled martensitic transformation during the crystallization and cooling of welded joints or during their loading. Deformation conversion of the microheterogeneous structure of MSA into disperse martensite is accompanied by the following synergistic effects. First, an increase in the share of the martensitic phase in the structure leads to an increase in hardness. Secondly, the energy of the external load, which is applied to the surface, is dissipated due to the micro-TRIP effect of deformation martensitic transformation. It causes the relaxation of microstrains within the surface layers. Thirdly, due to structural transformations, straines in the weld seam decrease. Therefore, while subjecting the MSA metal to external influences, there is a significant effect of enhancing the properties by implementing the internal resource of the material itself.

E. Estrin et al carried out experiments to evaluate external loads corresponding to the start of strain induced martensitic transformation. The quantity of strain induced martensite increases linearly when the external load threshold is reached. The magnitude of the strain is proportional to the initial quantity of the martensite in the sample. At straines exceeding the threshold value, the quantity of deformation martensite increases linearly with increasing straines. For steel 50N9X5, the value of the threshold level increases from 1000 to 2500 MPa with an increase in the initial amount of martensite from 15 to 75%. Similar results were given by M. Filippov for MAS steels.

According to A. Gulyaev, martensitic transformation occurs at an extremely high rate, approximately 10^{-7} s. This is faster by about an order of magnitude than the time of the most dynamic external mechanical influences.

MSA materials are marked by low cost of alloying, high resistance against wear (abrasive, erosive, cavitation, etc.) and other external influences. Our investigations showed that they are successfully used as hardfacing layers at surfacing and thermal spraying.

To provide the MSA structure in the welds of high-strength medium-alloy steels, we developed economically alloyed cored wire of the 50Cr18 type and the appropriate welding technology. The chemical composition of the alloy was chosen basing on the Fe-Cr-C system according to the Potak-Sagalevich diagram, corrected by Korolev and Pimenova. It allows predicting the phase composition of alloys with an allowable accuracy. The necessary C / Cr ratio was chosen from the following conditions:

$M_S \approx 20$ °C; $M_D > M_S$,

where M_S is a starting temperature of the martensitic transformation under cooling; M_D is a temperature of the martensitic transformation under deformation.

When the condition is satisfied, the martensitic transformation passes to a relatively small degree under cooling, while under loading it develops considerably. The data concerning an influence of alloying elements on positions of the martensitic points was taken from Filippov's monography. Along with the basic structural components, metastable austenite and martensite, it is also desirable to have a certain amount of ferrite as a relaxing layer improving the weldability and carbides to improve wear resistance.

The aim of the work was to analyze the features of the phase transformations occurring during crystallization and subsequent thermal and deformation effects during the loading of welds with the MSA structure.

1. Materials and research methods

Samples were prepared by arc welding / surfacing with the following parameters: shielding gas Ar-CO_2 82-18 mixture; cored wire of the 50X18 type with a diameter of 1.2 mm; current 200 A, voltage 34 V, welding velocity 22 m/h. Surfacing on a substrate of steel 1020 was performed in three layers with a total height of 12-15 mm. Then the coupons were cut from welded metal, Fig. 1. The purpose of the samples is shown in Table. 1.

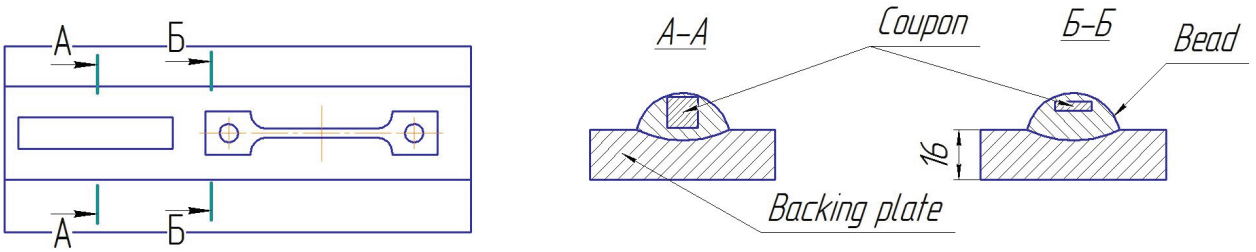

Fig. 1 Scheme of cutting the coupons

Table 1 Purpose of samples

№	Samples	Purpose
1	Cross section A-A, 10x10x50 mm	Abrasive wear test
2	Cross section Б-Б, length 75 mm, 3x3 mm in the operating part	High-temperature metallographic studies
4	1 mm from the surface, 10x10x10 mm	Shock and static ball loading

Tests on the propensity to cold cracking were carried out by rigid probe evaluation, adopted at a number of Russian machine-building enterprises, Fig. 2. Two plates150x300x13 mm from steel 30HGSA (0.3 C, 1.1 Cr, 1.0 Mn, 0.025 S, 0.025 P) were installed on a thick backing plate of steel 1020 and the plates were welded around the total perimeter. The bevel butt joint, beveling angle 40°, was made in three passes, Fig. 2.

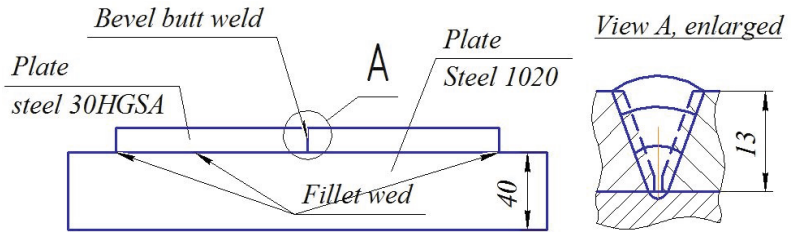

Fig. 2 Sample for cold cracking test

After 24 hours, the joint was checked for cracks by ultrasonic inspection and color flaw detection. Coupons for X-ray diffraction studies and the hardness evaluation were prepared from the welds along the joint cross-section.

Samples № 1, table 1, were subjected to a two-body abrasive test via the pin-on-plate reciprocating technique. Corundum abrasive paper with a grain size up to 150 μm was fixed on the plate and the sample was fixed in a holder. The test conditions were as follows: sliding distance 30 m; pin velocity 0.16 m/s; and specific load 1 MPa. To reduce the lapping period during the wear tests, the sprayed work surface area, 10 mm × 10 mm, on the pin was polished to Ra 0.8. A combination of corundum microhardness 22.900 MPa and a specific load of 1 MPa provide the scratching abrasive wear. This type of test was chosen for the following reasons:

- This type of wear is most easily reproduced in the laboratory and can be easily unified. Therefore, reference data on the relative wear resistance of various materials are comparable;
- Other types of abrasive wear (hydro- and gas-abrasive, shock-abrasive, and thermal-abrasive ones) also realize the same kind of surface failure with applying additional loads. As pointed by D.Garkunov and V. Belyi, the

row of relative wear resistance, obtained with scratching abrasive wear, is reproduced in other types of abrasive wear if microcutting is the main mechanism of surface failure during wear.

Comparison of abrasive wear resistance was carried out for austenitic steel DIN 110G13L used for wear parts of mining equipment, perlite steel like DIN 41Cr4, used for crowns of teeth of excavator buckets and 50Cr18 welds of MSA structure.

As shown in the charter Introduction, to begin the deformation martensitic transformation, it is necessary to apply external loads of 1000-2500 MPa. The experiments of L. Odintsov showed that the residual plastic deformation is expressed in the size of the impression (d), the value of which is directly proportional to the applied load and inversely proportional to the hardness of the metal. In this case, the depth of the hardening zone (h) is proportional to the depth of the impression well (h_1). Thus, the value of the hardness in the well corresponds to the degree of hardening of the metal from the static load from the spherical indenter, Fig. 3.

Experiments were carried out with the spherical indentor for quasistatic and dynamic loading of the sample No. 4, Table. 1, after equalizing grinding.

Quasistatic loading was performed for 50Cr18 and 41Cr4 alloys on a Brinell press, at a loading rate of $1 \cdot 10^{-3}$ m/s, and a spherical indentor of 5 mm in diameter (hereinafter HB indentor). The loads were 500 and 1000 kg, which corresponds to specific loads of 550 and 1100 MPa. Dynamic loading was performed by dropping a weight of 1 kg from a height of 1.2 m onto a 8 mm diameter ball of hard alloy BK8 GOST 3882 (WC-Co 92-8, hardness 87.5 HRA) placed in the center of the face of the 50X18 alloy sample of the sample № 4, table 1.

In the case of impact loading of 50Cr18 weld sample, a 2.4 mm diameter well was formed on the surface, which corresponds to the area S = 4.52 mm^2. At the weight of 1 kg a shock pressure will be 2170 MPa

To ensure an accurate hit of the weight on the ball, the fall of the weight was carried out within a pipe whose inner diameter is 2 mm larger than the diameter of the weight.

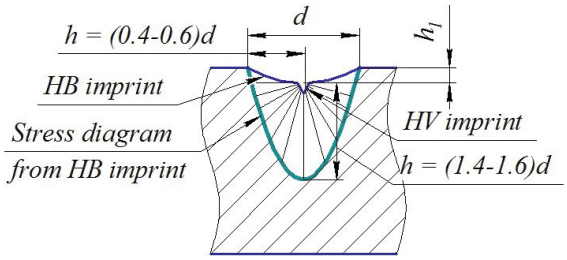

Fig. 3 Scheme of comparative evaluation of hardening

Measurement of the microhardness of the weld metal before and after loading was performed according to the scheme given in the table 2. As seen, specific loads exceed the value of starting martensite deformation threshold.

Table. 2 Scheme of microhardness measurements

Parameters	Quasistatic loading	Dynamic loading
Specific load from HB indentor, MPa	550, 1100	2750
The sample material	50Cr18, 41Cr4	50Cr18
The initial hardness of the weld metal	400 HV	37 HRc
Measurement area	Center of the well*	Line**

* deviation from the center of the bottom of imprints was ± 0.5 mm
** is carried out on the surface of the sample along the axis of the well from the HB indenter

The features of structural transformations in the conditions of welding thermal deformation cycles were studied using high-temperature metallographic installation ALA-TOO (Plant of Instrumentation, Frunze, USSR). It allows to study strain relaxation under the influence of the martensitic $\gamma \rightarrow \alpha_M$ transformation directly in the process of elastic-plastic deformation. According to the method of B. Potekhin, samples No. 2, table 1, of 50Cr18 and 41Cr4 alloys with attached thermocouples were heated by running current in vacuum. After achieving 900 °C, the current

was switched off and unfixed samples cooled for 3-4 seconds. When the temperature drops to 450 °C, the specimens were rigidly fastened by rapid stretching to a strength of 50 MPa (below the yield point) using an electromechanical drive. During the subsequent cooling, the length of the samples did not change. Rapid cooling caused an elastic deformation and an increase in strains. Its value corresponds to the thermal compression of the samples to a certain level, after which a sharp drop in strain was associated with the development of the martensitic transformation.

Microhardness was measured with a PMT-3 device (LOMO, St. Petersburg, Russia) under a 100 g load. The structure was studied with a MET 2 microscope (Altami, St. Petersburg, Russia), Phase composition on the surface was determined by a XRD-7000 X-ray diffractometer (SHIMADZU, Kyoto, Japan, Cr-Kα radiation). The following survey conditions were used: radiation - Cu Kα, graphite monochromator, 2θ angular range 30-100 °, scanning step 0.04 °, and exposition period at the point - 3 sec. An electron microscopic study of the structure of thin foils of the 50Cr18 alloy was carried with EVL-100 electronic transmission microscope (plant of electron microscopes, Sumy, USSR).

3 Results and its discussion

3.1 Evaluation of weldability

Color flaw detection of butt welds in the rigid probe did not revealed any cracks, fig. 4fig. Ultrasonic inspection also did not detected the cracks in the butt welds.

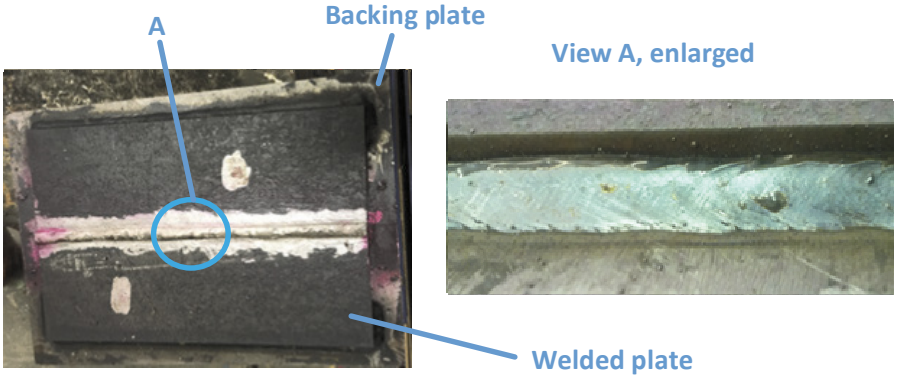

Fig. 4 Color flaw detection of the butt weld in a rigid probe

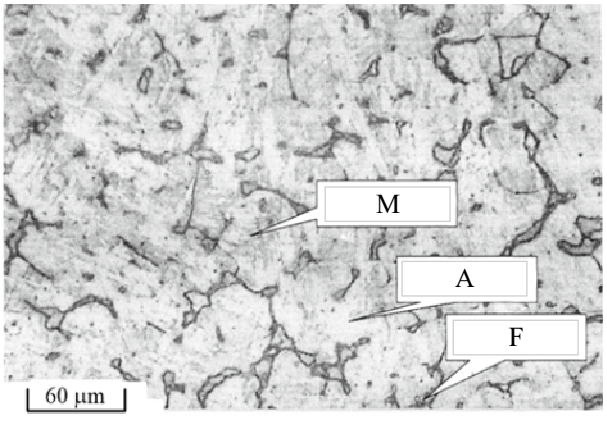

Fig. 5 The microstructure of a 50Cr18 weld in the depth of 2 mm from the surface

3.2 Structure study

After etching with chloroazotic acid the microstructure of the sample of alloy 50Cr18 consist of a conglomerate

of grains varying by color and microhardness (HV_{50}). It includes the following: light yellow austenite (A) grains, 3000 MPa; dark herbaceous groups of martensite (M) plates, 4850 MPa, inside the A grains, and bright white precipitates of δ-ferrite (F) along the boundaries of A grains, 2000 MPa; fig. 5.

Diffractograms obtained from samples before wear are shown in Fig. 6. As seen, the predominant phases are austenite with the presence of twins, also α-martensite crystals are present in some areas of austenite (fig. 6a). Split dislocations, fig. 6b, indicates a low stacking fault energy of austenite. Sections of δ-ferrite have a round shape with a dislocation substructure, fig. 6c.

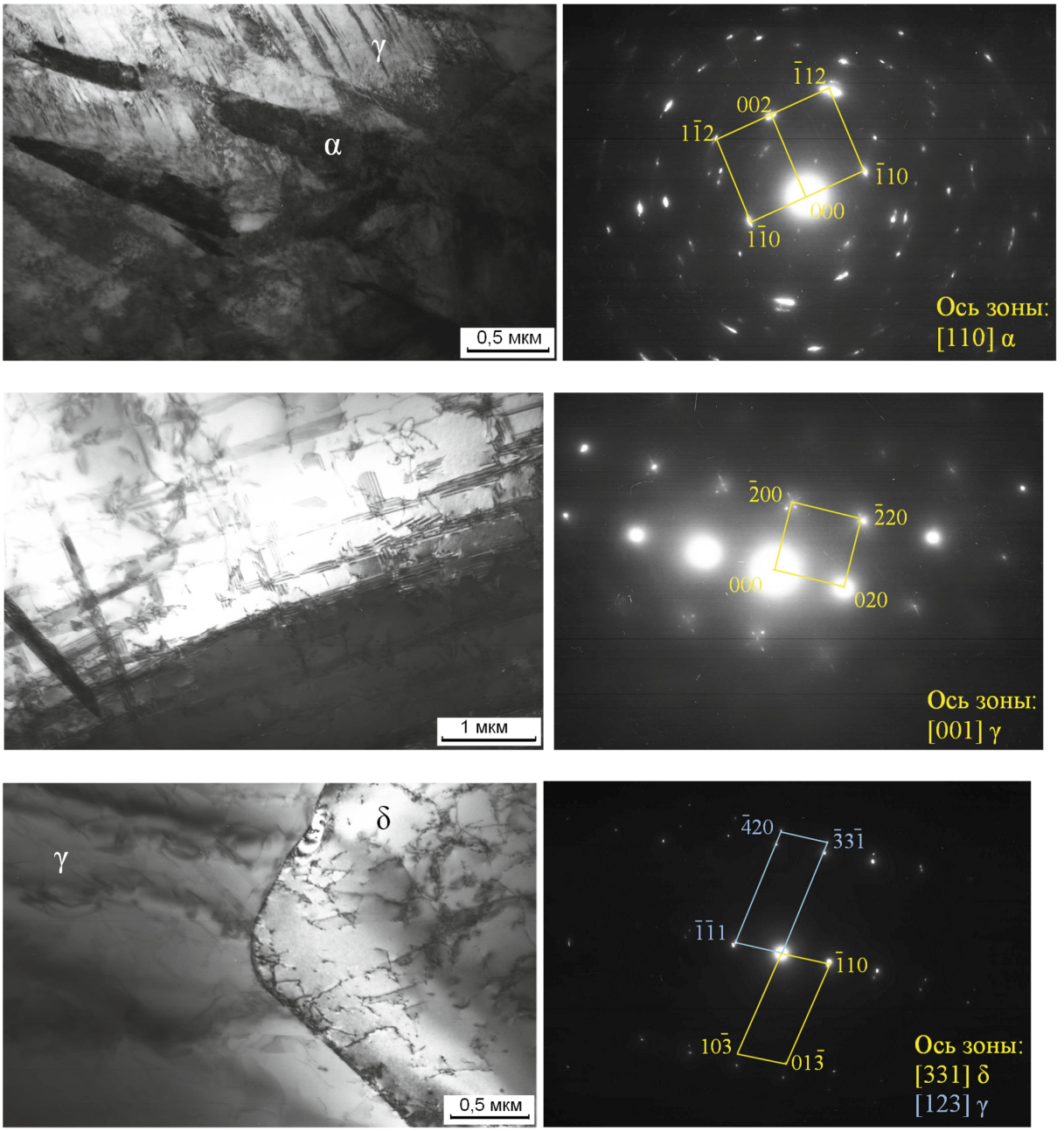

Fig. 6 The structures of thin foils of the alloy 50Cr18. On the left - structure, on the right - decoding scheme. a - austenite and α-martensite; b – indication low stacking fault energy of austenite; c - δ-ferrite of round shape.

3.3 Analysis of mechanical effects

Microhardness after quasistatic loading, increases at the bottom of the well as the load of HB indenter increases due to an increase of the deformation degree.

Table. 3 Hardness at the bottom of the well from the HB indenter

Steel	Load, kg		ΔHRC_{50} 0	ΔHRC_{100} 0
	500	1000		
Steel 50Cr18; air cooling after welding, HRC32	51	55	19	23
Steel 41Cr4; normalization 860 °C, average tempering at 500 °C, 2 h, HRC37	44	47	7	10

As seen from table 3, the increase in hardness of steel 50Cr18 is more than twice as high comparing to steel 41Cr4. It is explained by substantial contribution of strain induced martencitic transformation to the increase in hardness. In 41Cr4 steel, the increase in hardness occurs mainly due to the perlite hardening.

After dynamic loading by ball impact the hardness on the well surface was higher comparing to static loading. The difference is reasoned by higher specific load at the first case, see table 2. A sharp change of hardness in the well of 50Cr18 weld confirms strain induced martensitic transformation, fig. 7.

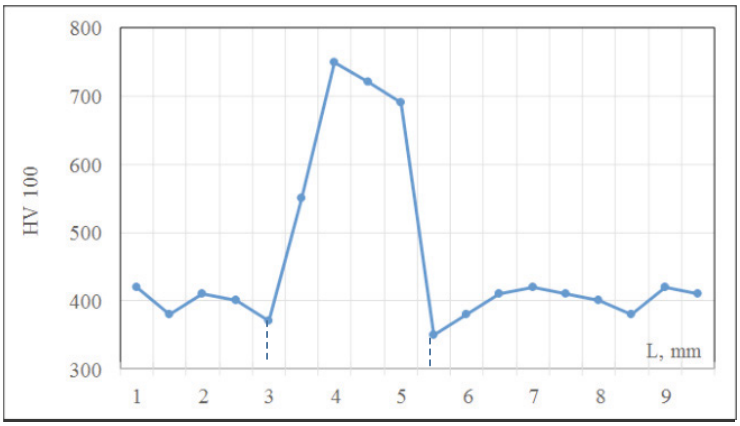

Fig. 7 Microhardness of the surface of steel 50Cr18 weld, along the axis of the well after ball impact

The weight loss of 50X18 weld samples after tribological tests was 0.38 g. Comparison was done with 41Cr4 and 110G13 steels. The results showed that the wear resistance of 50Cr18 weld is higher comparing to the examined alternatives, table 4.

Table 4 Comparison of examined materials by relative weight loss.

Material	Relative wear resistance
50Cr18 weld	1.46
41Cr4 steel	0.79
110G13L steel	1

According to the X-ray diffraction analysis, the samples from the 50Cr18 weld contain 3 phases: A, F, and M with a body-centered tetragonal lattice, fig. 8 and table 5.

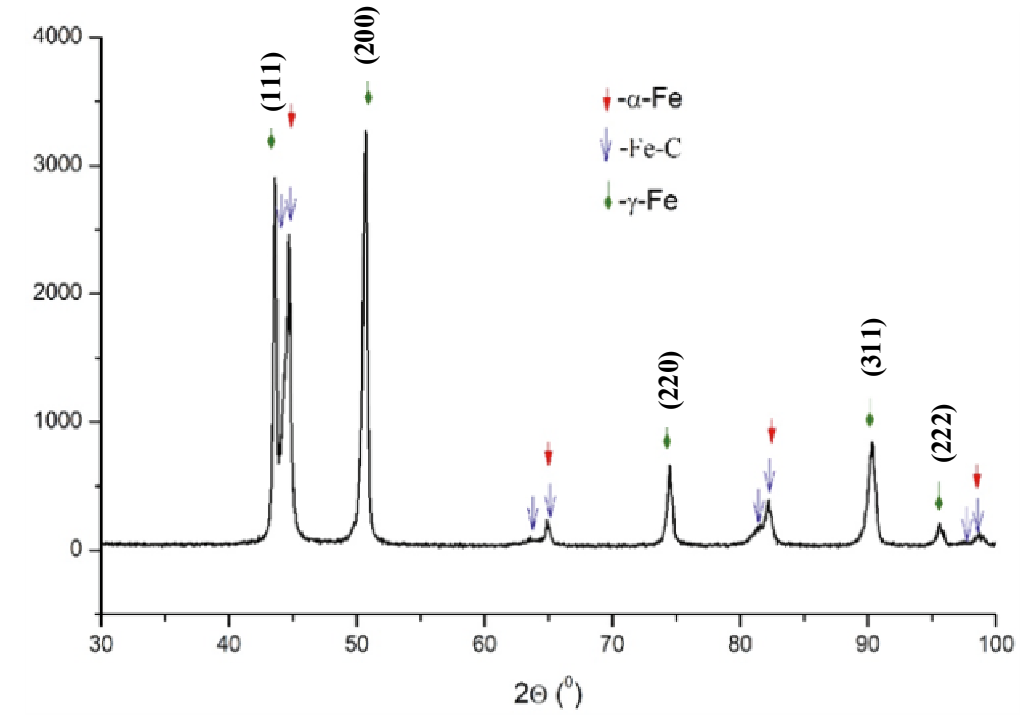

a

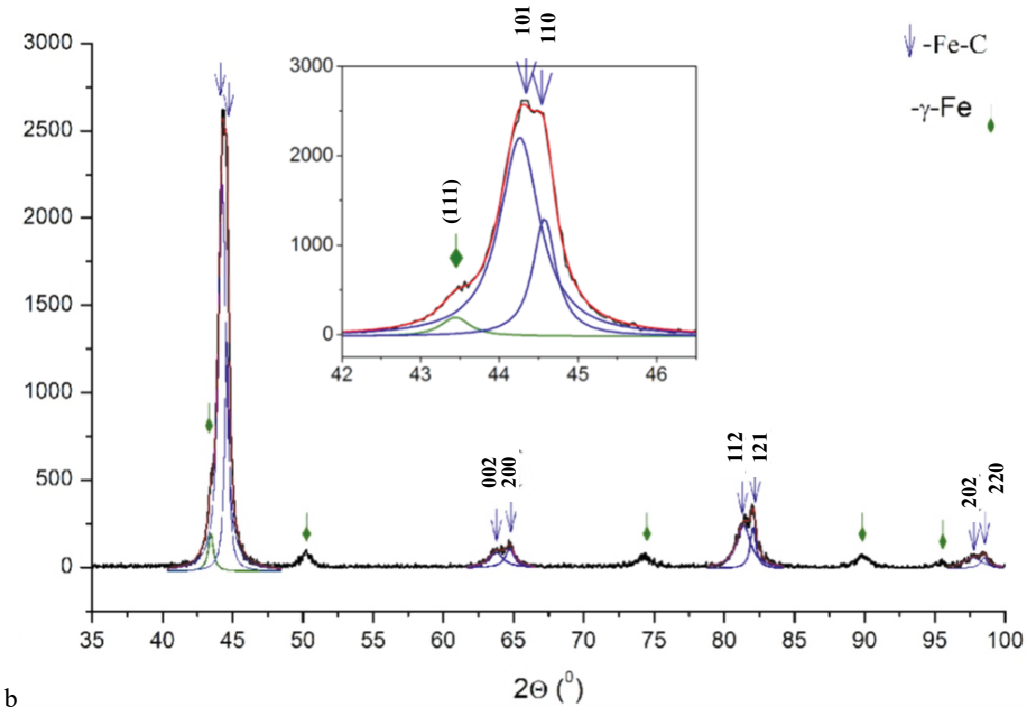

b

Fig. 8 Diffractograms of a working surface of 50Cr18 alloy: the initial (a); after wear (b)

Precise determination of the percentage of phases is difficult due to the strong texturing of the austenite and superposition of the peaks of the ferrite and martensite phases.

Although the X-ray diffraction analysis did not reveal carbides, they are present with high probability due to the high content of C and Cr. As pointed by M. Goldstein, difficulties in detecting are caused by small dimensions of secondary carbides.

An approximate calculation of the area of the diffraction peaks suggests that before loading austenite share was about 50 %, and martensite phase is half of austenite. After the abrasion test, the martensite amount was noticeably higher than the amount of residual austenite, which remained approximately 15%. Most of metastable austenite, about 35%, was converted to martensite in the surface layer. A decomposition of some diffraction peaks into components corresponds to the phases in the sample, see fig. 8b.

Table 5 Phase composition and parameters of the cell before and after abrasive wear of 50Cr18 weld

Surface condition	Phases	Dimension, Å, and volume, Å^3, of crystal lattice (number of peaks)			
		a, Å	c, Å	c/a	V, Å^3
Initial	F	2.8712 (9)	n/a	n/a	23.67 (2)
	A	3.602 (1)	n/a	n/a	46.8 (4)
	M	2.870(1)	2.901(4)	1.011(2)	23.9 (3)
After abrasive wear	F+M	2.875(1)	2.907(2)	1.011(1)	24.03(3)
	A	3.612(2)	n/a	n/a	47.14(8)

3.4 Strain relaxation analysis

The features of the formation of strains of the first kind in the samples № 2, table 1, of 50Cr18 weld and 41Cr4 steel are shown in fig. 9. As seen, rapid cooling caused an elastic deformation and an increase of strains to a certain level, after which a sharp decrease in the strains, associated with the development of the martensitic transformation, occurred. The nature of the curves for both alloys is fundamentally similar: the increase in straines occurs up to the point M_D. Then the relaxation process begins, developing in a certain temperature range, after which the strains again increase. The level of the strain after the martensitic relaxation is lower in case 50Cr18 weld. But less inclination angle of the next strain rise during cooling leads to a lower final strain in this case. The maximum strain was 200 MPa at 250 °C, and 115 MPa at 150 °C for 41Cr4 steel the 50Cr18 weld, correspondingly. Taken cooling rate was the same as at typical welding processes. Therefore, using 50Cr18 weld reduces the risk of cold cracking. Additionally, δ-ferrite precipitates along the boundaries of the austenite grains. It is a place for martensite transformation developing. It also reduces cold cracking risk in case of 50Cr18 weld.

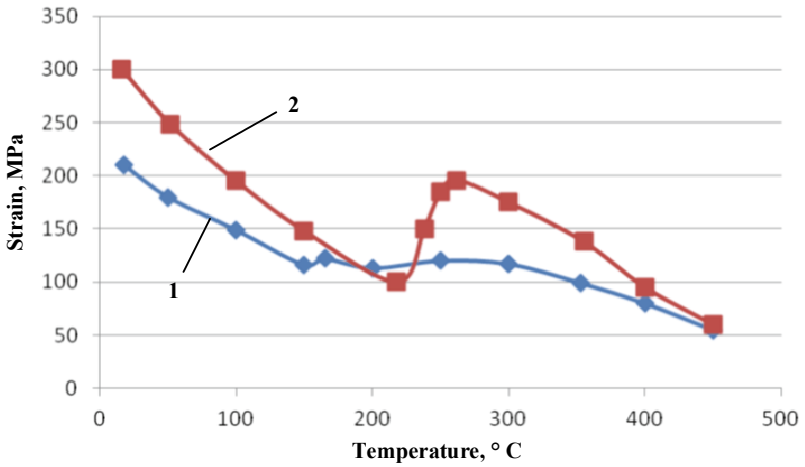

Fig. 9 The strain magnitudes in the process of cooling of the fixed samples from 50Cr18 weld (1) and 41Cr4 steel (2)

As shown, the martensitic transformation does not end above room temperature in the 50Cr18 weld. Therefore,

its important feature is the relaxation of thermal and phase macro-strains in rigidly fixed weld structures.

Conclusions

1. Phase transformations at crystallization and subsequent thermal and deformation effects under loading were studied applying to the welds from economically alloyed cored wire of 50Cr18 type. It is shown that the weld metal has a high capacity for intensive hardening in the process of local deformation action and good abrasive wear resistance. These features are reasoned by TRIP effect due to heterophase structure of the weld metal, containing metastable austenite, δ-ferrite and martensite.

2. Another positive effect of metastable austenite presence is lower strain level after cooling. Therefore, it reduces cold cracking risk in comparison with ferrite-pearlitic steels.

Acknowledgments

The authors would like to thank B. Potekhin, S. Estemirova, E. Korzunova, M. Tyumkova, B. Stroganov for assistance in structure studies.

References

Belyi V.; Ludema K., Myshkin N., 1994. Tribology in the USA and the Former Soviet Union; Allerton Press: New York, NY, USA.

Bogachev, I., Mintz. R., 1959. Cavitation Destruction of Iron-Carbon Alloys, In: Mashgiz, Moscow-Sverdlovsk, pp. 111.

Davydov Yu. , Korobov Yu., Davydov A., 2018. Estimation of the Parameters of Pulse-Arc Welding with a High-Chromium Cored Wire. Welding Production, 6, 14-20.

Filippov, M., Litvinov V., Nemirovski, Yu., 1988. Steels with Metastable Austenite. In: Metallurgy, Moscow, pp. 256.

Garkunov, D.N. Tribotechnics (Wear and Wear-Free State), 2001. MSKHA: Moscow, Russia.

Goldstein, M., Grachev, S., Veksler, Yu., 1999. Special Steels, 2d edition. In: MISIS, Moscow, pp. 408.

Gulyaev, A., 1982. Superplasticity of Steel. In: Metallurgy, Moscow, pp. 56.

Gulyaev, A., 1986. Metal Science. In: Metallurgy, Moscow, pp. 544.

Korobov, Yu., Filippov, M., Shymiakov V., Verkhorubov, V., Nevezhin, S., Legchilo V., Hydorozhkova, Yu., 2013. Metastable Chromatic Austenite as a Structure Factor of Improving Wear Resistance of Deposited Metal and Sprayed coatings, p. 40-46. In: Cherniak, S. (Ed.). Metal Scientists and Metallurgists, IGUPS, Irkutsk, pp. 312.

Korobov, Yu., Verkhorubov, V., Nevezhin, S., Filippov, M., Tkachuk, G., Makarov, A., Zabolotskikh, I., 2016. An Influence of Strain-Induced Nucleation of Martensitic Transformations on Tribological Properties of Sprayed and Surfaced Depositions. International Thermal Spray Conference and Exposition ITSC 2016, Shanghai, China, 694-699.

Korolev, N., Pimenova, O., Boronenkov, V., 2002. Method of Numerical Estimation of Phase Content and Structure of Wear Resistant Hardfacing Materials. Welding Production, 4, 11-16.

Lippold, John C., 2015. Welding Metallurgy and Weldability. In: John Wiley & Sons, Inc., XVIII, pp. 401.

Makarov, E., Yakyshin, B., 2014. Theory of Weldability of Steels and Alloys. In: Makarov, E. (Ed.). MGTU, Moscow, pp. 474.

Odintsov, L., 1987. Strengthening and Elaborating of the Parts by Surface Plastic Deformation. In: Mechanical Engineering, Moscow, pp. 328.

Olson, G. B., Cohen, M. A., 1972. Mechanism for the Strain-Induced Nucleation of Martensitic Transformation, J. of the Less-Common Metals, 28, pp. 107-118.

Potak, Ya., 1972. High Strength Steels. In: Metallurgy, Moscow, pp. 208.

Potekhin, B., 1979. Physics of Metals and Metal Science, 48, 5, 1058-1076.

Schastlivtsev V., Filippov, M., 2005. Role of the Bogachev - Mints Concept of Metastability of Austenite in Choosing Wear-Resistant Materials. Metal Science & Heat Treatment 47, 1/2, 3-5.

Volchenko, V., Makarov, E, Ship, V., et al, 1991. Welding and Welded Materials: in 3 vol. Vol. 1 Weldability of Materials. A Reference book. In: Makarov, E. (Ed.). Metallurgy, Moscow, pp. 528.